# Photon Funnel Design Based on Spatially Variant Self-Collimating Photonic Crystals

Noel P. Martinez<sup>1</sup>, Chun Xia<sup>2</sup>, Stephen M. Kuebler<sup>2,3,4</sup>, and Raymond C. Rumpf<sup>1</sup>

<sup>1</sup>EM Lab, Department of Electrical and Computer Engineering, University of Texas at El Paso, El Paso, TX 79968, USA

<sup>2</sup>CREOL, The College of Optics and Photonics, University of Central Florida, Orlando, FL 32816, USA

<sup>3</sup>Chemistry Department, University of Central Florida, Orlando, FL 32816, USA

<sup>4</sup>Department of Material Science and Engineering, University of Central Florida, Orlando, FL 32816, USA

Author e-mail address: rcrumpf(autep.edu

**Abstract:** We present a device that flows a beam incident at any position and angle along the input side of a lattice to a single zone at the output. We report the performance of the device. © 2021 The Author(s)

### 1. Introduction

Spatially-variant photonic crystals (SVPCs) are periodic structures that are bent, twisted, or otherwise spatially varied to achieve an optical function while minimizing deformation of the unit cells to preserve optical properties of the lattice, like self-collimation [1]. Self-collimation is a phenomenon observed in photonic crystals where light is forced to propagate along a specific direction within the lattice without diffracting. Self-collimating SVPCs have unlocked a vast domain of possibilities for new optical devices. They have been used to control the beam direction at both microwave and optical frequencies [2,3], and more recently, to control multiple properties of light at the same time [4]. In this work, we demonstrate a photon funnel design based on self-collimating SVPCs. Numerical simulations show that the photon funnel collects light incident at any position and angle along the input and directs it towards a concentration zone at the output.

## 2. Device Design, Results, and Discussion

The photon funnel design, shown in Fig. 1(a), is composed of  $60\times60$  unit cells with lattice spacing a. The unit cell used for this design is described in [5]. To evaluate the optical performance of the device, we performed numerical simulations using the finite-difference frequency-domain (FDFD) method [6,7]. We used a Gaussian beam source with a wavelength of  $\lambda_0 = a/0.4831$  and a beam width of  $w = 4\lambda_0$ . We calculated the insertion loss (IL) by integrating the Poynting vector at the right side of the simulations with and without the photon funnel present and calculating their ratio.

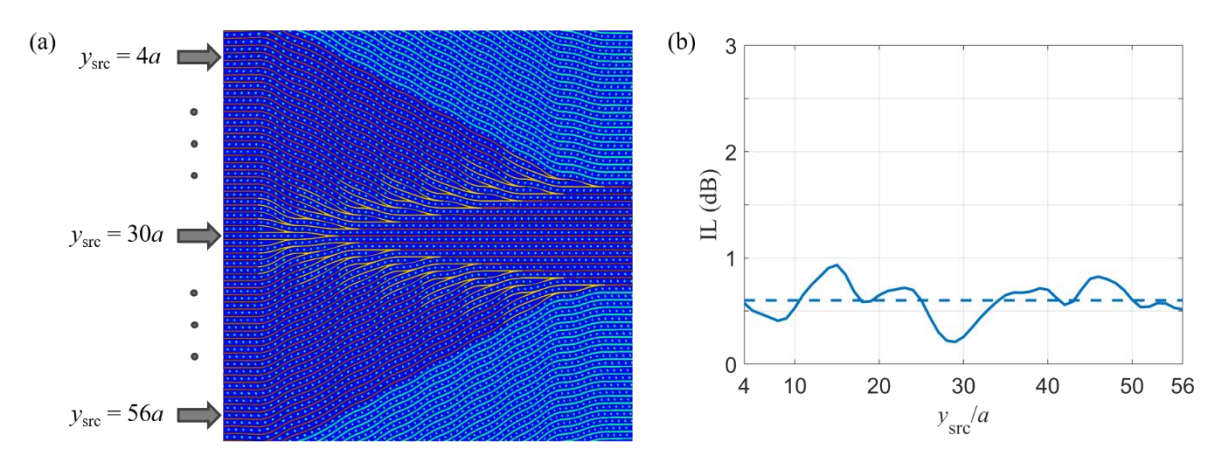


Fig. 1. (a) Photon funnel design for a 60×60 unit cell lattice. The arrows along the left side depict the source at different positions along the input side of the lattice. The concentration zone, located along the center of the lattice at the output side, is 15 unit cells wide. (b) Insertion loss calculated by varying the position of the source along the input side of the photon funnel. The average insertion loss (dashed line) is only 0.6 dB.

For the first test, we varied the position of a source at normal incidence from the top of the lattice  $(y_{src} = 4a)$  to the bottom of the lattice  $(y_{src} = 56a)$ , as depicted by the arrows in Fig. 1(a). The results of this sweep are given in Fig. 1(b), where the average insertion loss (IL = 0.6 dB) is denoted by the dashed line. It is clear that this design performs very well no matter the position of the source. The simulations in Fig. 2 show the fields for three cases.

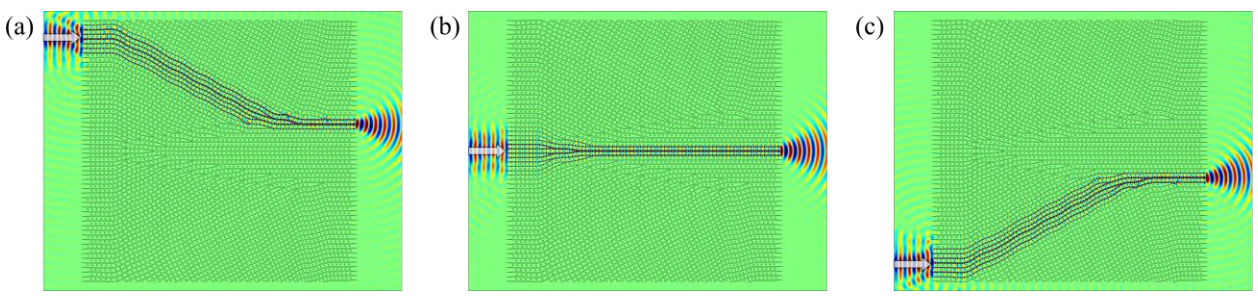


Fig. 2. Electric fields from FDFD simulations of the photon funnel. (a) The source is incident at  $y_{src} = 4a$  and the insertion loss is IL = 0.58 dB. (b)  $y_{src} = 30a$  and IL = 0.26 dB. (c)  $y_{src} = 56a$  and IL = 0.52 dB.

To calculate the angular acceptance of the photon funnel, we performed an angle sweep between  $\pm 15^{\circ}$ . For each angle, we varied the position of the source from the top of the lattice to the bottom of the lattice and calculated the average insertion loss. The results, given in Fig. 3(a), show that the insertion loss remains below 3 dB for incident angles  $|\theta_{\text{inc}}| \le 12^{\circ}$ .

Next, we calculated the fractional bandwidth (FBW) of the photon funnel by setting  $\theta_{inc} = 0^{\circ}$  and performing a wavelength sweep between  $0.85 \le \lambda_{inc}/\lambda_0 \le 1.20$ . The results, plotted in Fig. 3(b), show that this design has an insertion loss less than 3 dB for wavelengths between  $0.88 \le \lambda_{inc}/\lambda_0 \le 1.17$ . This gives an impressive FBW of 29%.

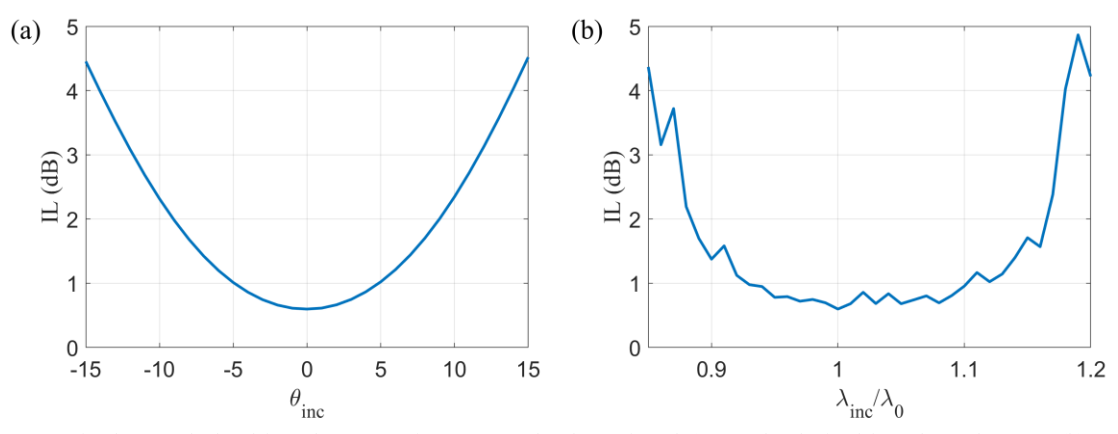


Fig. 3. Insertion losses calculated from the parametric sweeps on the photon funnel. (a) Results obtained from the angle sweep. (b) Results obtained from the wavelength sweep.

## 3. Summary

In conclusion, we demonstrated a photon funnel design that flows a beam incident at any position and any angle at in the input face to a concentration zone at the output face with an average insertion loss of only 0.6 dB. The FBW of this device is calculated to be 29% and the angular acceptance is  $|\theta_{inc}| \le 12^{\circ}$ .

#### 4. Acknowledgements

This project was supported in part by NSF grants 1711529 and 1711356.

#### 5. References

- [1] R. C. Rumpf and J. Pazos, "Synthesis of spatially variant lattices," Opt. Express 20(14), 15263-15274 (2012).
- [2] R. C. Rumpf, J. Pazos, C. R. Garcia, L. Ochoa, and R. Wicker, "3D printed lattices with spatially variant self-collimation," Progress In Electromagnetic Research, Vol. 139, 1-14 (2013).
- [3] J. L. Digaum, J. J. Pazos, J. Chiles, J. D'Archangel, G. Padilla, A. Tatulian, R. C. Rumpf, S. Fathpour, G. D. Boreman, and S. M. Kuebler, "Tight control of light beams in photonic crystals with spatially-variant lattice orientation," Opt. Express 22, 25788-25804 (2014).
- [4] J. J. Gutierrez, N. P. Martinez, and R. C. Rumpf, "Independent control of phase and power in spatially variant self-collimating photonic crystals," J. Opt. Soc. Am. A 36, 1534-1539 (2019).
- [5] R. E. Hamam, M. Ibanescu, S. G. Johnson, J. D. Joannopoulos, and M. Soljačić, "Broadband super-collimation in a hybrid photonic crystal structure," Opt. Express 17, 8109-8118 (2009).
- [6] R. C. Rumpf, "Simple implementation of arbitrarily shaped total-field/scattered-field regions in finite-difference frequency-domain," Progress In Electromagnetic Research B, Vol. 36, 221-248 (2012).
- [7] R. C. Rumpf, C. R. Garcia, E. A. Berry, and J. H. Barton, "Finite-difference frequency-domain algorithm for modeling electromagnetic scattering from general anisotropic objects," Progress In Electromagnetic Research B, Vol. 61, 55-67 (2014).